Riley Winebarger
May 1, 2018

Mapping Sinkhole Susceptibility of Northwestern Arkansas

Problem Statement

How accurate is digitally mapping sinkhole susceptibility, and how do different methods compare?

Method for Testing

Create a sinkhole susceptibility map of northwest Arkansas using biomass, soil thickness, vegetation root depth, precipitation and geologic units, compare the areas of high susceptibility to known sinkhole locations in the Ozarks. Create a map of potential sinkhole locations based on proximity to fault and streams features as well as type of geologic unit. Compare this map to known sinkhole formations and compare the two analysis methods to determine which is more accurate.

Hypothesis

It is predicted that sinkhole formations will be more dependent on biomass, vegetation, and soil thickness than distance from streams and faults. This is because soil and biomass characteristic are likely more important in determining potential sinkhole formations than relative locations.

Introduction

Karst landscapes are difficult to understand for a variety of reasons. One aspect that makes karst especially challenging is locating it due to its high heterogeneity. New advancements have given rise to digitally predicting and identifying karst features such as sinkhole formations. There are many different ways in which data can be processed to identify karst features.

Vegetation and biomass have been used to characterize karstic features as well as rock type and proximity to streams and faults. Weight of the land has also been used as well as head gradient, potentiometric maps and contour lines. China has fairly recently begun to successfully delineate karst features using airborne Lidar and vegetation types. This new version of identifying karst features is efficient considering China has 3.44 million km^2 of karst areas. Which makes up 36% of total land area in China and 15.6% of all the 22 million km^2 of all karst areas in the world (Jiang et al., 2014). Land area in China is subject to land degradation, due to harsh land practices and easily susceptible land. Forests in China are especially easy to degrade when habits begin to become destroyed by human disturbances. Rock desertification is a common occurrence in southwest China, regions underlain with soluble rock, having thin soil layers and little vegetation become subject to weathering and erosion exposing rocky terrain (Wang et al. 2004; Jiang et al. 2014). This term has been coined rocky desertification and leads to karst features such as sinkholes forming relatively quickly when coupled with harsh land practices (Shi-jie 2002).

There are many different ways to predict and quantify sinkhole formations. Digitally predicting sinkholes is becoming more important in areas such as southwestern China, Florida, and parts of Arkansas and even Texas, as karst collapses quickly and at times unpredictably. This investigation focuses on sinkhole formation prediction based on both relative locations and by quantifying land, soil, and precipitation values.

Data Collection

SSURGO data and water base layer data were all collected from the Arkansas state GIS Office (gis.arkansas.gov). The water base layer containing stream and river information was published by Arkansas Department of Environmental Quality and uses the GCS North American 1983 spatial coordinate system. SSURGO data was sourced from the U.S. Department of Agriculture, Natural Resources Conservation Service and the National Soil Survey Center. SSURGO data was collected and published in 2013 and used NAD 1983 projected by UTM Zone 15N. The SSURGO contained soil data of Northwest Arkansas, data was not precise enough to show high variability of soil type over very short distances. SSUGRGO soil data was used in determining soil thickness and root depth. Geologic units, faults, and dikes were sourced from USGS mineral resource data from the United States Geological Survey in 2000. These three datasets all used the GCS North American 1927 spatial coordinate system. Biomass data was published by the National Renewable Energy Laboratory in August of 2017. The data uses GCS North American 1983 spatial coordinate system. Biomass data was downloaded as a feature class for the entire United States. Because the data was for the entire US, data quality was poor when clipped to Arkansas, containing only about 50 cells for the entire state. Climate data which contained annual average precipitation and temperatures of 2010 came from Natural Resources Conservation Service Arkansas. The data was presented in a CSV file containing latitude and longitude measurements in decimal degrees. Sinkhole data was found for the Ozark Plateaus of Northern Arkansas from the USGS Lower Mississippi-Gulf Water Science Center that digitized sinkhole polygons from USGS topographic maps over the Ozark Plateaus Physiographic Province of northern Arkansas. The data used historical (1940s through 1980s) and more recent (2014) topographic maps in the creation of the dataset. The data used a projected coordinate system of USA Contiguous Albers Equal Area Conic USGS version.

Data Preprocessing

Climate data was converted from CSV form to point features in ArcGIS by specifying XY data of longitude and latitude in decimal degrees, GCS North American 1983 spatial coordinate system was used. Once the events were created the trend tool was used to convert the point features to a raster. This raster was created based on annual precipitation averages for 2010 in centimeters. SSURGO data was interpolated using the metadata to determine which column head acronym indicated vegetation roots depth and soil thickness. Once that was determined, a raster was created for both root depth and soil thickness using the “Feature to Raster” tool. The

geology units were also converted to a raster using the “Feature to Raster” tool and delineating by “Rock Type”. Biomass was clipped to just the state of Arkansas then converted to a raster with values based on total biomass using “Feature to Raster”. All rasters including the water base layer feature which included river and streams were then clipped to the root depth and soil thickness extents, this region was used as the study area (Figure 1), because it covers the Northwestern portion of the state where most Ozark sinkhole features were located. Clipping the data to a smaller size allowed more detail to be shown and to increase processing speeds. Clipping the data to this size also allowed for the data to be more centralized on the known locations of sinkholes in the Ozarks (Figure 2).

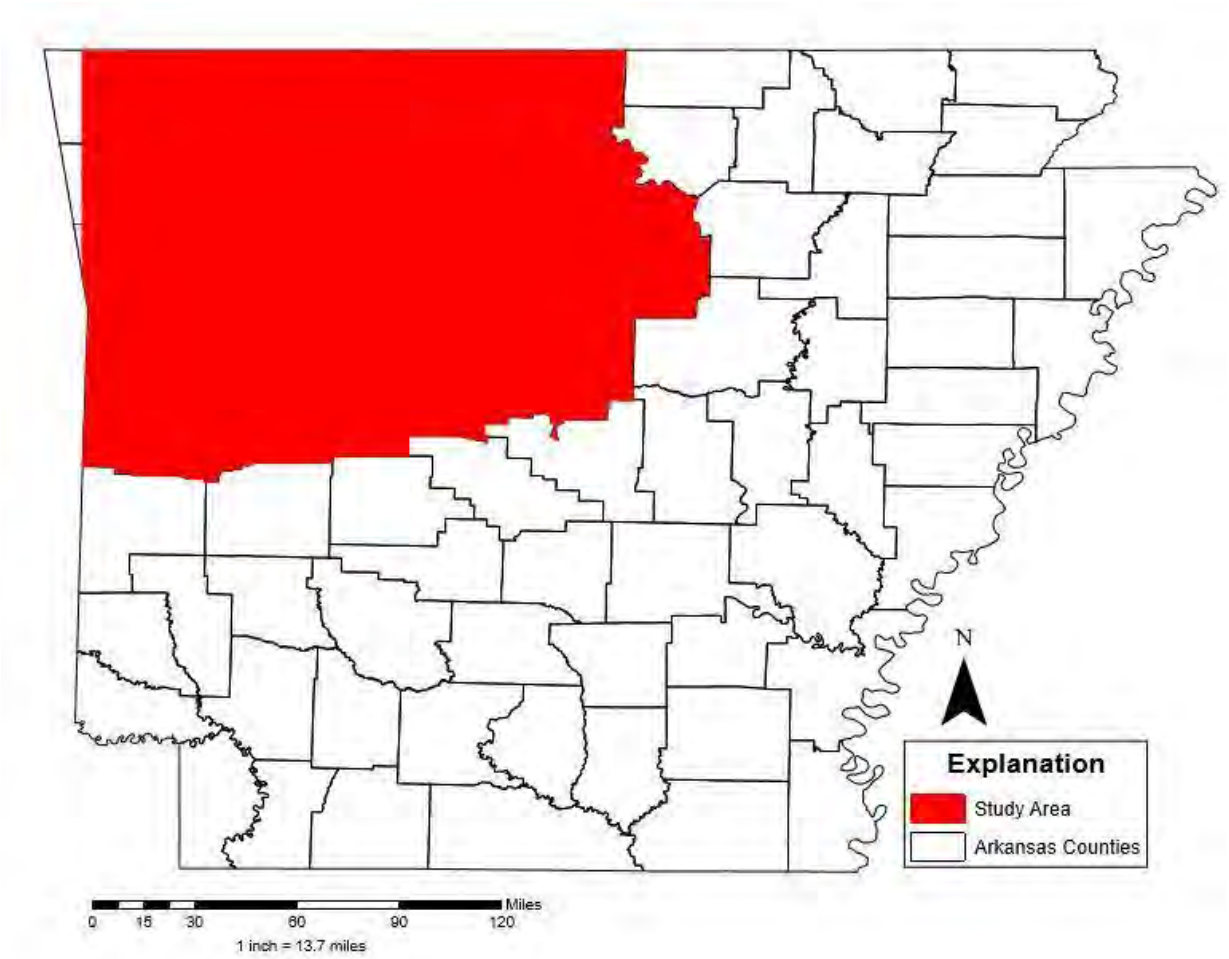

Figure 1. Sinkhole susceptibility study area of northwest Arkansas.

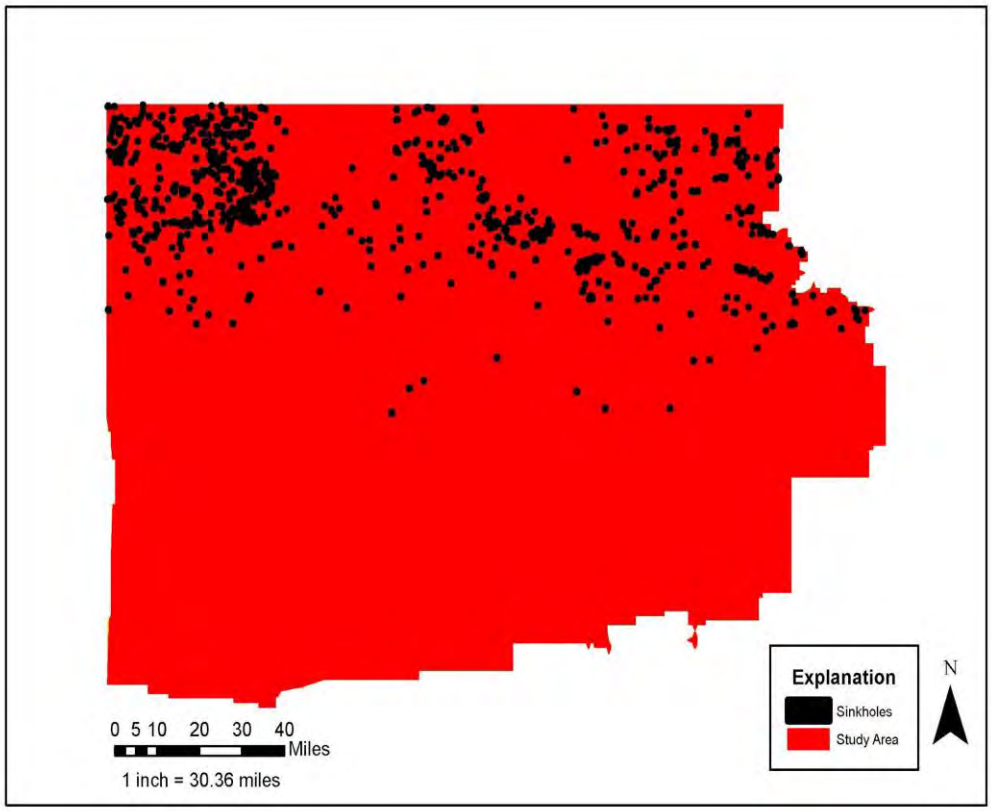

Figure 2. Known sinkhole locations located inside the study area.

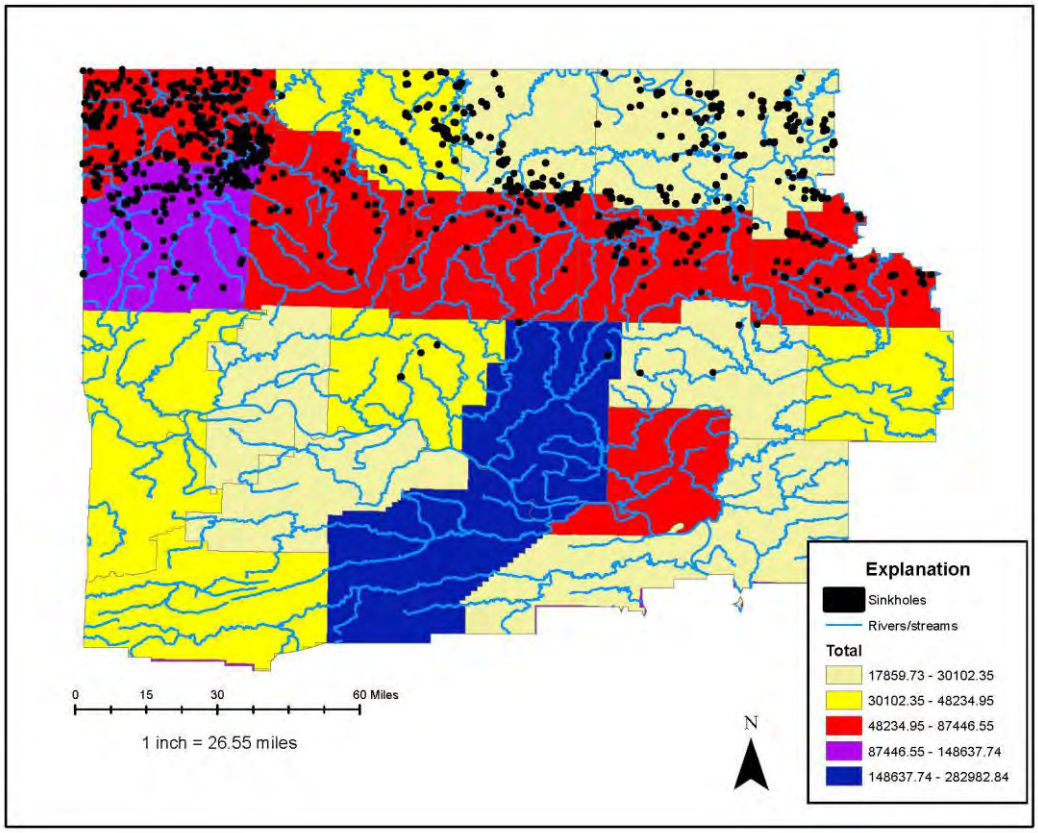

Figure 3. Biomass values in the study area data from National Renewable Energy Laboratory (2017).

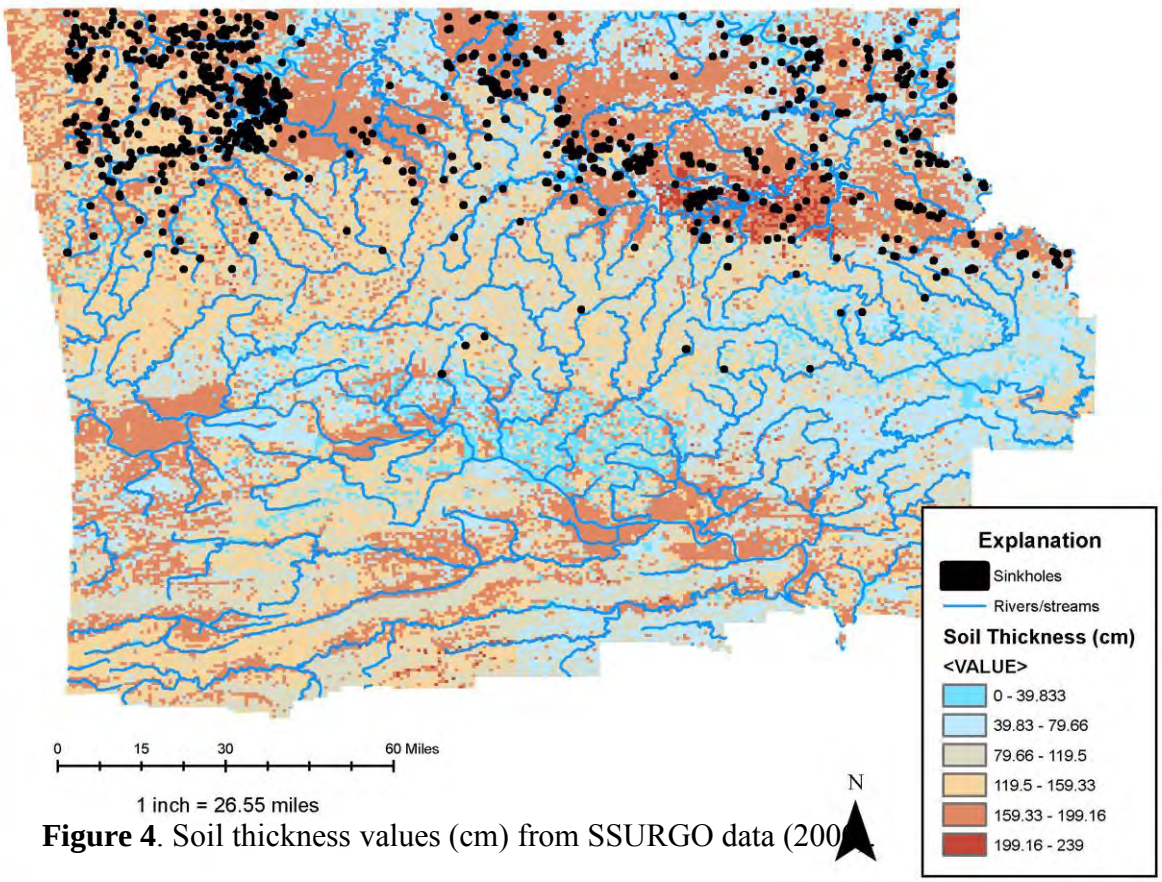

Figure 4. Soil thickness values (cm) from SSURGO data (200

Figure 5. Root depth (cm) from SSURGO data (2000).

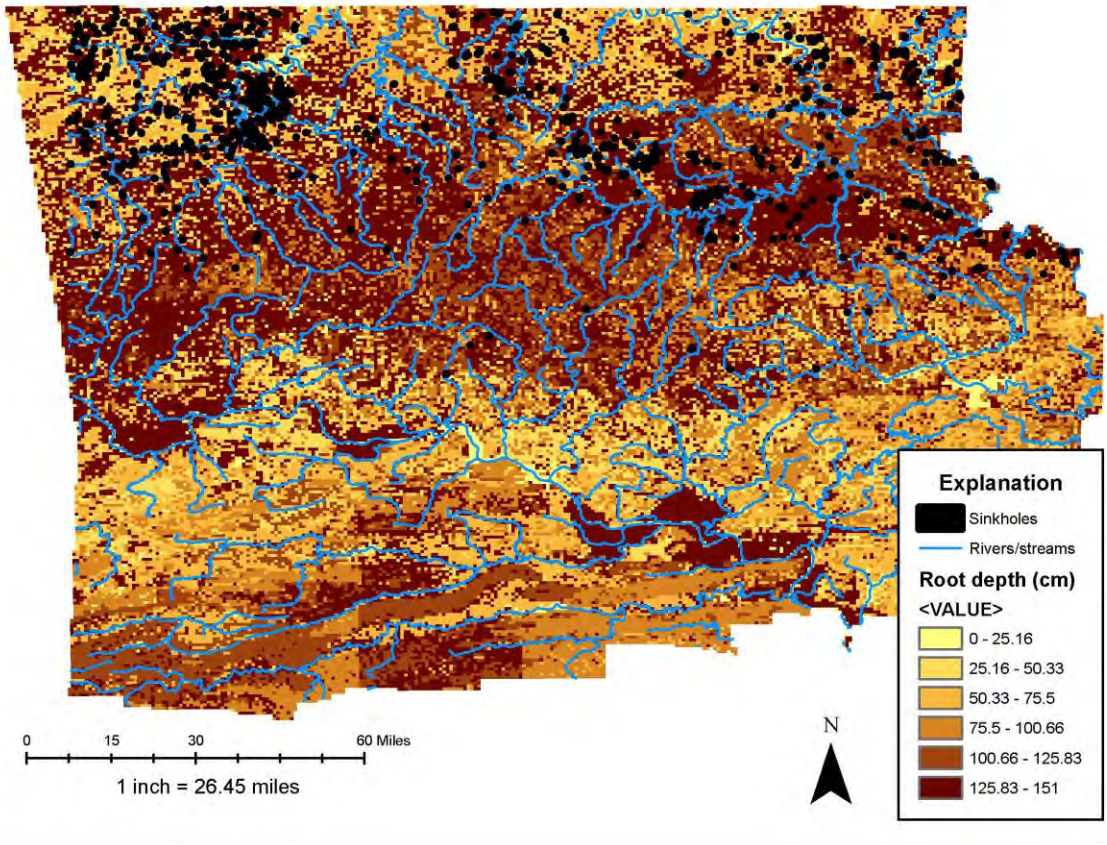

Data Processing and Analysis

In order to determine sinkhole susceptibility, biomass, soil properties, precipitation averages, and rock type rasters were used to create a susceptibility map. These rasters were first reclassified using the "Reclassify" tool. Reclassifying was done as indicated by Table 1-5. Reclassifying was executed with the knowledge that sinkholes form in soluble rock such as limestone and dolomite. Sinkhole formation is also most favorable in areas with low above ground biomass, shallow root depth (Ni 2015 found 89% of roots in the first ~20cm of soil in sinkhole prone areas), thin soil layer, and high average precipitation values. Once reclassified lower values were indicative of more sinkhole susceptible areas while higher values were areas less likely to form sinkholes.

Table 1. Reclassified Values of Geologic Units

Rock Type	Reclassified Value
Limestone	1
Dolostone (dolomite)	1
Shale	9
Sandstone	3
Alluvial Terrace	3
Alluvium	3
Sand	6
Water	9
Clay/mud	9
Novaculite	7
Chert	8
Gabbro	8
Alkalic Intrusive Rock	8

Table 2. Reclassified Soil Thickness Values	
Soil Thickness (cm)	Reclassified Values
0 - 26.555556	1
26.555556 - 53.111111	2
53.111111 - 79.666667	3
79.666667 - 106.222222	4
106.222222 - 132.777778	5
132.777778 - 159.333333	6
159.333333 - 185.888889	7
185.888889 - 212.444444	8
212.444444 - 239	9

Table 3. Reclassified Root Depth Values	
Root Depth (cm)	Reclassified Values
0 - 16.777778	1
16.777778 - 33.555556	2
33.555556 - 50.333333	3
50.333333 - 67.111111	4
67.111111 - 83.888889	5
83.888889 - 100.666667	6
100.666667 - 117.444444	7
117.444444 - 134.222222	8
134.222222 - 151	9

Table 4. Reclassified Biomass Values	
Total Biomass	Reclassified Values
17859.73 - 19268.51	1
19268.51 - 26478	2
26478 - 35874.83	3
35874.83 - 48234.95	4
48234.95 - 66090.64	5
66090.64 - 87446.55	6
87446.55 - 123321.98	7
123321.98 - 148637.74	8
148637.74 - 282982.84	9

Table 5. Reclassified Precipitation Values	
Precipitation (cm)	Reclassified Values
47.032307 - 47.954823	1
47.954823 - 48.561699	2
48.561699 - 49.145985	3
49.145985 - 49.72979	4
49.72979 - 50.314072	5
50.314072 - 50.897877	6
50.897877 - 51.482159	7
51.482159 - 52.089035	8
52.089035 - 53.011925	9

Once all rasters had been reclassified, the susceptibility map was created (Figure 6). This was performed using the "Raster Calculator" and weighing each of the rasters equally. This produced a raster with values from 9 to 39, lower values were more indicative of sinkhole susceptible areas. A red to green color symbolism was used to symbolize the newly created raster. River and stream data overlaid this raster for context as well as known sinkhole locations.

To determine how accurate the susceptibility map was, the raster was converted to a polygon. Values less than 20 were selected using the "Select by Attribute" tool. From there, the "Select by Location" tool was used to determine where known sinkhole locations intersected the values less than 20. There were a total of 944 known sinkhole locations, only 207 sinkholes were found to intersect with values less than 20. That only accounts for 21.9% of the total sinkhole values. That percentage is too low to give an accurate prediction on sinkhole susceptibility. However, only the northern section of the map has values of known sinkholes. The entire northwest portion of Arkansas was used, though known sinkhole values only account for a small portion of the map, in effort to show trends in the calculated raster. The known locations of sinkhole formations were digitized from historical (1940s through 1980s) and more recent (2014) topographic maps in the creation of the dataset. The older topographic maps had the majority of sinkholes in the northern portion of the study area while more recent (2014) topographic maps showed sinkhole formations primarily in the south/southeast and central regions of the study area. Thus, it is plausible that sinkhole susceptibility areas are changing with time in northwestern Arkansas and the south is becoming increasingly susceptible to sinkhole formations that have yet to either occur or be mapped. This is made more plausible by biomass, precipitation, and geology data sets being younger than many of the known sinkhole formation location data points.

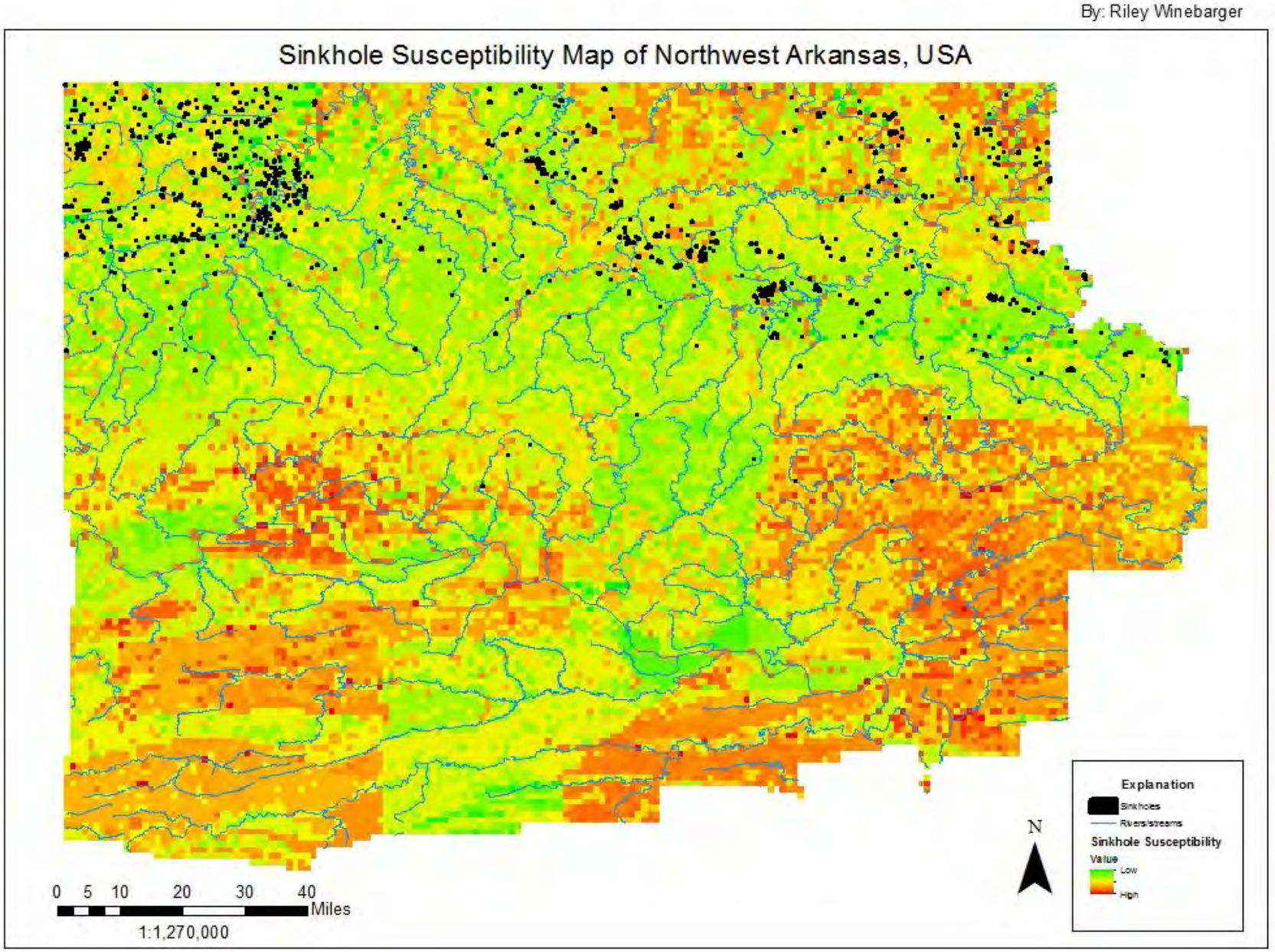

Figure 6. Sinkhole susceptibility map of northwest Arkansas based on biomass, root depth, soil thickness, precipitation, and geology data.

Another analysis was performed to quantify the presence of sinkholes based on proximity to fault lines, distance from streams, as well as the type of rocks. This analysis was based on an investigation in 2005 of Shenandoah Valley, Virginia that correlated sinkhole formations to proximity of stream and faults as well as rock type. The study found sinkholes to be sporadic near streams and more abundant 600 to 1400 feet away from streams then decline with distance away. Sinkholes were most abundant in Ordovician aged carbonate rocks. Sinkholes were also most common 1000 feet away from faults (Hyland, 2005). This analysis was mimicked for the northwest Arkansas region but did not prove correlation like the Shenandoah Valley study.

Buffers were created around input features of faults and streams, using the "Buffer" analysis tool. A buffer was created 1000 feet away from all fault lines. Zero values of known sinkhole locations were within 1000 feet from fault lines. Perhaps rock type overshadowed proximity to faults for sinkhole formations. The "Select by Location" function was used to determine if any known sinkholes were within the region 1000 feet away from faults. Sinkhole correlation to streams was also weak. Buffers were created 600, 800, 1000, 1200, and 1400 feet from all streams. This was done using the same process as the fault lines buffer. Figure 7 and 8 display buffer surrounding the streams for the different intervals. The results from these buffered stream values are displayed in Table 6.

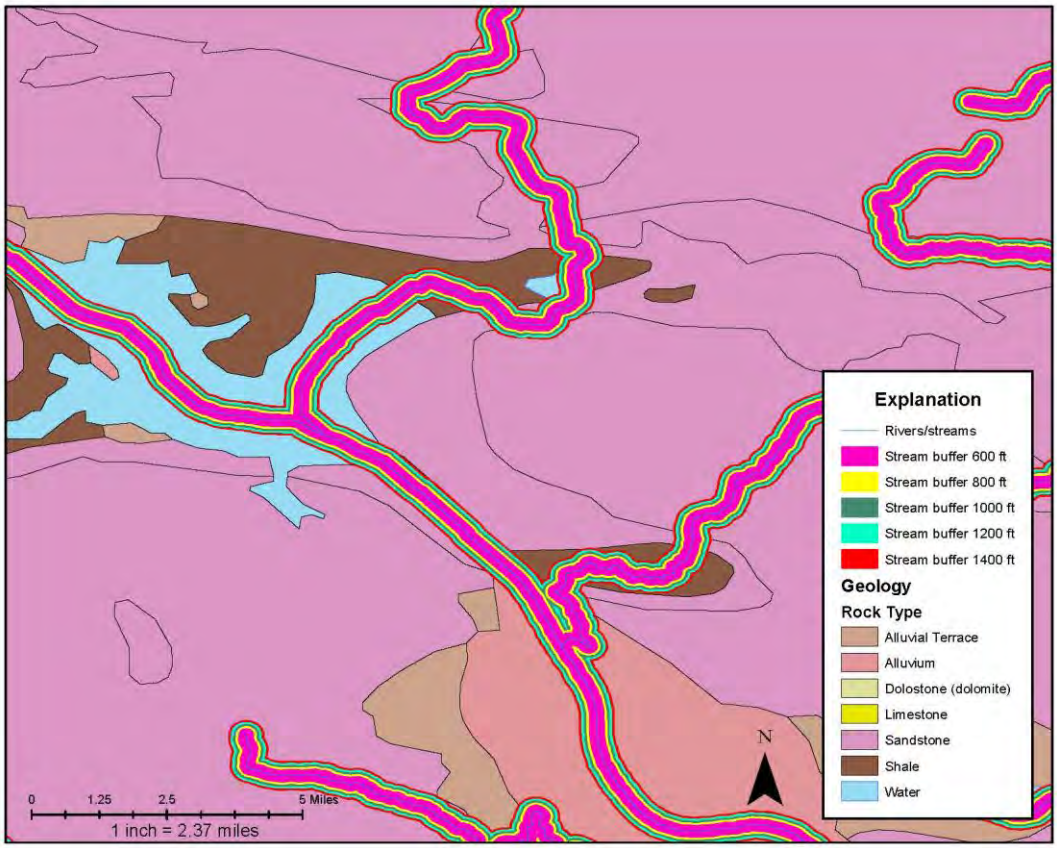

Figure 7. Close up of the buffer intervals around stream features.

Figure 8. Buffer intervals around stream features, full extent.

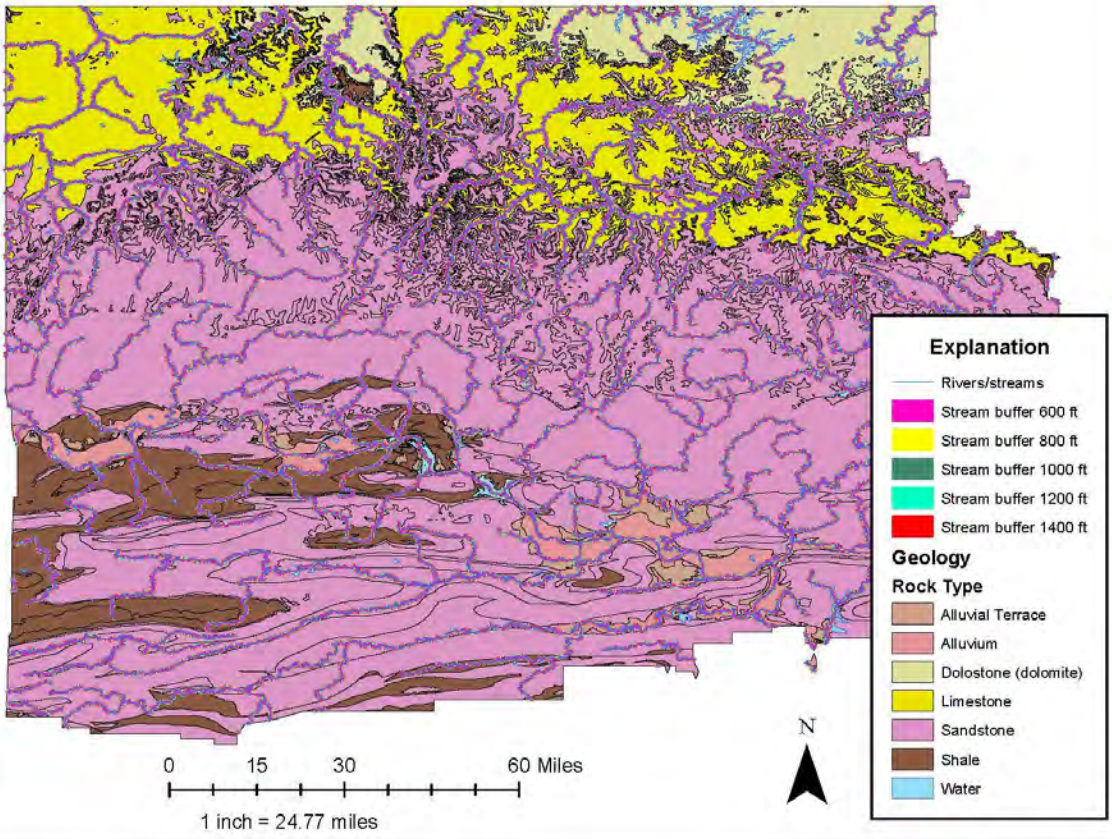

Table 7. Quantities of sinkholes found distances away from streams

Distance away from stream	Number of sinkholes
0 - 600 feet	27
600 - 800 feet	15
800 - 1000 feet	13
1000 - 1200 feet	15
1200 - 1400 feet	9
Total 600-1400 feet	52

Figure 9. Sinkholes found within 600 feet of stream features

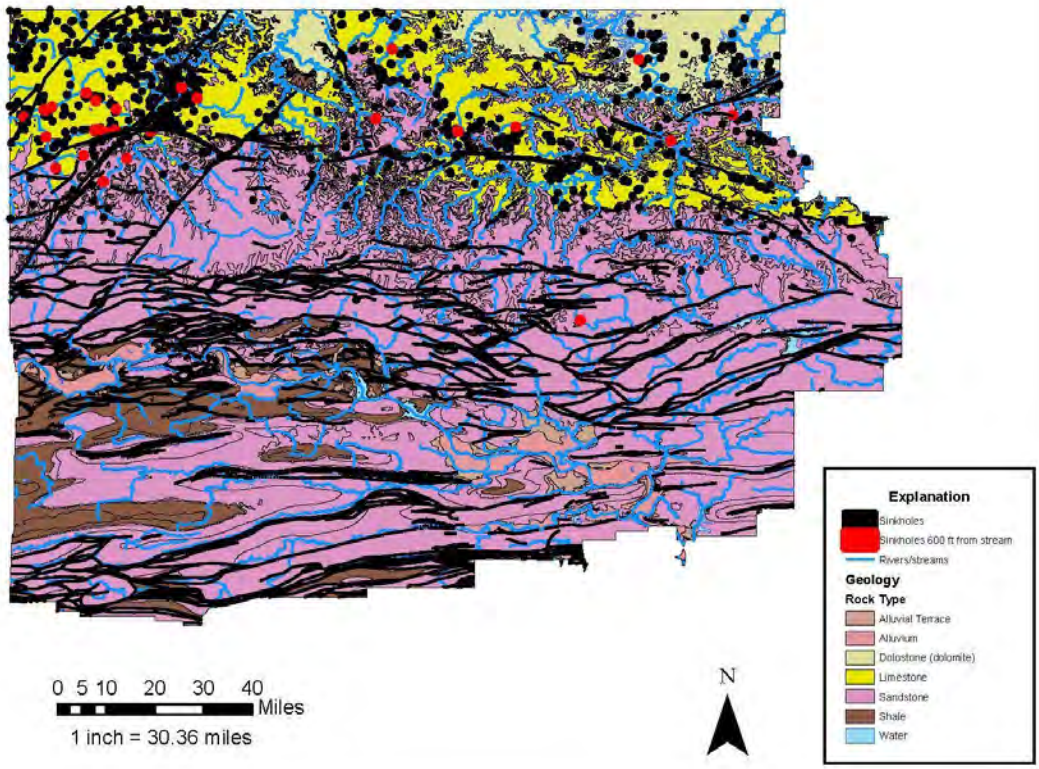

Figure 11. Sinkholes found within 800 feet of stream features

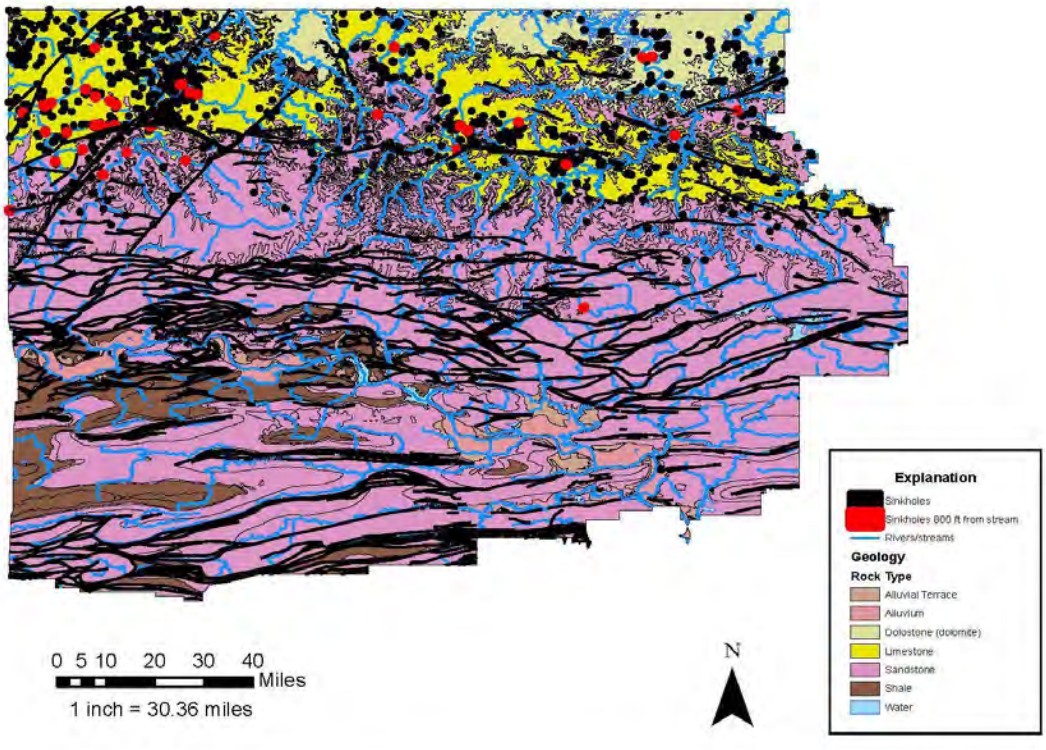

Figure 11. Sinkholes found within 1000 feet of stream features.

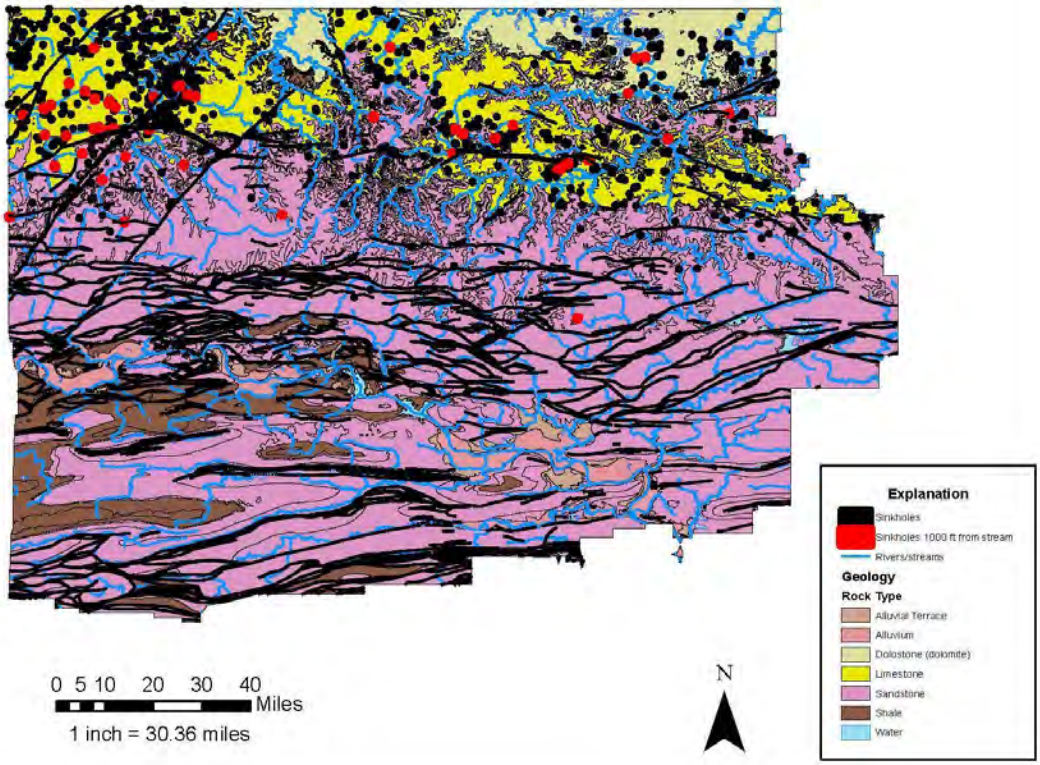

Figure 12. Sinkholes found within 1200 feet of stream features.

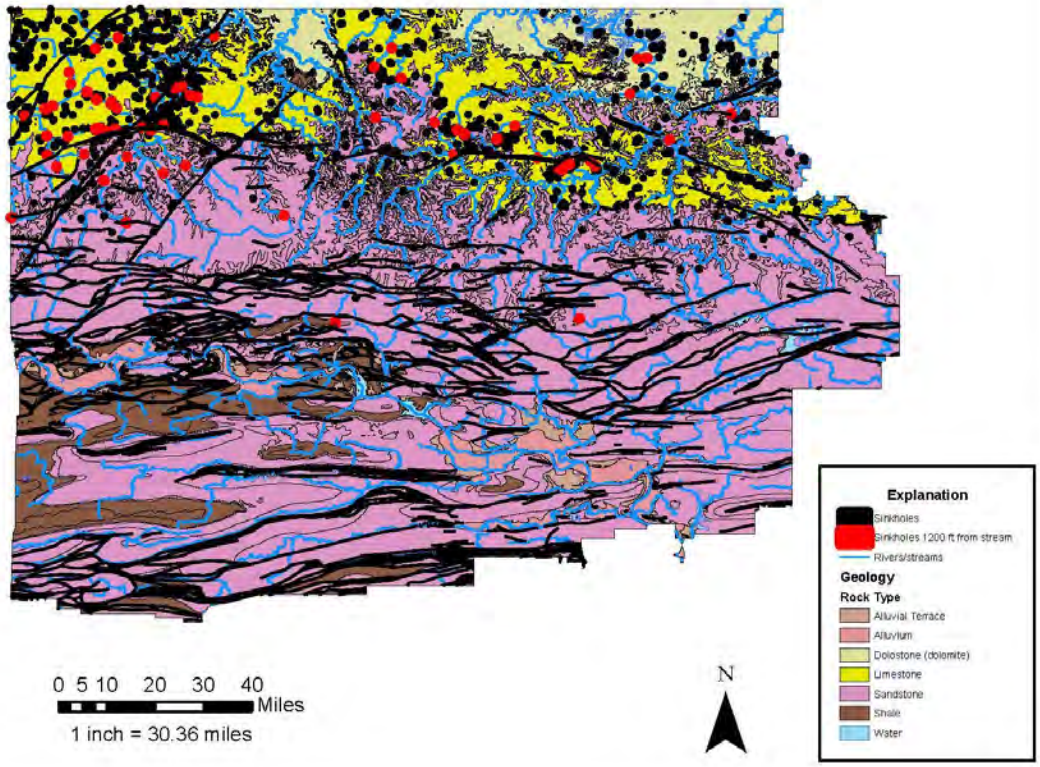

Figure 13. Sinkholes found within 1400 feet of stream features.

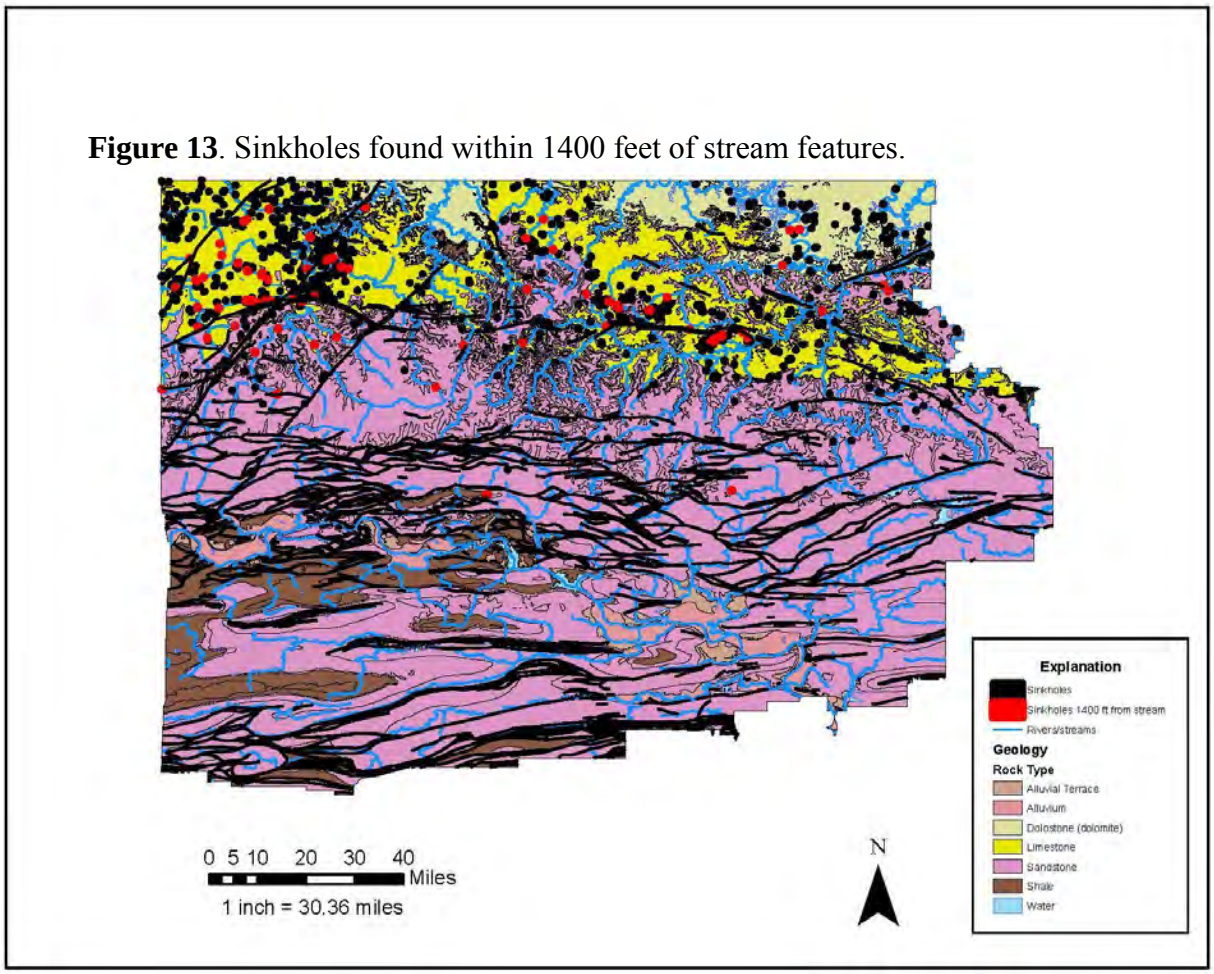

A total of 52 sinkholes found between 600 and 1400 feet of all streams is not a strong correlation, especially because there are 944 sinkholes total, meaning this accounts for just 5.5% of all sinkholes. 739 sinkholes were found within layers of limestone and dolostone, which is obvious because it is in soluble rock that sinkholes form. The remaining sinkholes were present in alluvium or sandstone layers. Alluvium deposits are likely just a thin deposit directly overlaying a soluble rock such as limestone or dolomite, and perhaps only surrounding sinkhole depressions. This alluvium present where the sinkholes form likely could have been eroded away, revealing limestone or dolomite where the sinkhole truly formed. This is possible because some of the sinkhole data is more recent (2014) than geologic units (2000), and alluvium deposits can be easily eroded away depending on thickness, or alluvium units could have been deposited around sinkholes after formation. Other remaining sinkholes not in limestone, dolomite, or alluvium, were present in the sandstone layer. This is plausible because the number of reported large-scale karstic features appearing in sandstone units are increasing (Alexander 2013; Young 1987). It is often disputed whether karstic features in sandstone are pseudokarst or true karst, it relies on the type of sandstone dissolution (Young 1987). More information is needed to confirm the presence of sinkholes in the sandstone units but it is likely they are represented correctly.

Discussion

Though the susceptibility map had a higher correlation to known sinkhole locations (21.9%), than proximity to faults and streams to the known sinkhole values (0% and 5.5% respectively), the correlation is still weak given data of known sinkhole formations; though, the argument has been made for its relevance in predicting future areas of susceptibility. This method should not be relied upon entirely for the region of northwestern Arkansas unless it is determined that more sinkholes begin to form in the southern portion of the study area. The southern portion of the study area shows the highest amount of sinkhole susceptibility and contains few relatively recent (digitized from 2014 maps) sinkhole formations, likely showing where new sinkholes will form in the future. For more reliable data and to determine the accuracy of this susceptibility map, this method could be coupled with other methods used to digitally predict and map sinkhole locations. Other methods include but are not limited to: identifying sink areas in DEMs from Lidar data, identifying areas of strong head gradient, and areas with vegetation common in karstic regions and sinkholes. Both data analysis processes used in this investigation should be tested in other sites since they have been reliable in other locations in the past. It could be that the Ozark sinkholes are dependent on a factor not included in this investigation.

Works Cited

Alexander, Scott C., et al. "Combining LiDAR, aerial photography, and Pictometry® tools for karst features database management." (2013).

Hyland, Sara Elizabeth. Analysis of sinkhole susceptibility and karst distribution in the northern Shenandoah Valley, Virginia: implications for low impact development (LID) site suitability models. Diss. Virginia Tech, 2005.

Jiang, Zhongcheng, Yanqing Lian, and Xiaoqun Qin. "Rocky desertification in Southwest China: impacts, causes, and restoration." Earth-Science Reviews 132 (2014): 1-12.

Kobal, Milan, et al. "Using Lidar data to analyse sinkhole characteristics relevant for understory vegetation under forest cover—case study of a high karst area in the Dinaric Mountains." PloS one 10.3 (2015): e0122070.

Ni, J., et al. "Vegetation in karst terrain of southwestern China allocates more biomass to roots." Solid Earth 6.3 (2015): 799.

Papadopoulou-Vrynioti, Kyriaki, et al. "Karst collapse susceptibility mapping considering peak ground acceleration in a rapidly growing urban area." *Engineering Geology* 158 (2013): 77-88.

Shi-jie, W. "Concept deduction and its connotation of karst rocky desertification [J]." *Carsologica Sinica* 2.2 (2002): 101-105.

Su, Zongming, and Xiankun Li. "The types of natural vegetation in karst region of Guangxi and its classified system." Guangxi Zhiwu 23.4 (2003): 289-293.

Wang, S.J., Liu, Q.M., Zhang, D.F., 2004. Karst rocky desertification in southwestern China: geomorphology, landuse, impact and rehabilitation. Land Degrad. Dev. 15, 115–121.

Wang, S. J., and Y. B. Li. "Problems and development trends about researches on karst rocky desertification." *Advances in Earth Science* 22.6 (2007): 573-582.

Young, R. W. "Sandstone landforms of the tropical East Kimberley region, northwestern Australia." *The Journal of Geology* 95.2 (1987): 205-218.